

A Measurement of the Parity Violating Proton Asymmetry in the Capture of Polarized Cold Neutrons on ³He

R. Alarcon^a, L.P. Alonzi^b, S. Baeßler^b, S. Balascuta^a, L. Barrón-Palos^c, J.D. Bowman^{d1}, J.R. Calarco^e, R. Carlini^f, C. Crawford^{g1}, N. Fomin^h, M.T. Gerickeⁱ¹, C. Gillis^j, G.L. Greene^h, V. Gudkov^k, G. Hale^l, A. Hayes^l, A. Klein^l, R. Mahurinⁱ, E. Martin^g, J. Martin^m, M. McCreaⁱ, J. Mei^j, M. Musgrave^h, S. Pageⁱ, S.I. Penttilä^d, A. Salas-Bacchi^l, P.-N. Seoⁿ, M. Viviani^o,

^a *Department of Physics, Arizona State University, Tempe, AZ 85287-1504*

^b *Department of Physics, University of Virginia, Charlottesville, VA 22904-4714*

^c *Department of Physics, Universidad Nacional Autónoma de México, México, 04510, México*

^d *Physics Division, Oak Ridge National Laboratory, Oak Ridge, TN 37831*

^e *Department of Physics, University of New Hampshire, Durham, NH 03824*

^f *Jefferson National Laboratory, Newport News, VA 12002*

^g *Department of Physics and Astronomy, University of Kentucky, Lexington, KY 40506*

^h *Department of Physics and Astronomy, University of Tennessee, Knoxville, TN 37996*

ⁱ *Department of Physics, University of Manitoba, Winnipeg, Manitoba, R3T 2N2 Canada*

^j *Department of Physics, Indiana University, Bloomington, IN 47408*

^k *Department of Physics and Astronomy, University of South Carolina, Columbia, SC 29208*

^l *Los Alamos National Laboratory, Los Alamos, NM 87545*

^m *Department of Physics, University of Winnipeg, Winnipeg, Manitoba R3B2E9, Canada*

ⁿ *Department of Physics, North Carolina State University, Raleigh, NC 27695-8202*

^o *INFN-Pisa, 56127 Pisa, Italy*

[the n-³He Collaboration]

2010-12-08

1. Introduction

This is an update to the n-³He PV experiment proposal, “A Measurement of the Parity Violating Asymmetry in the Capture of Polarized Cold Neutrons on ³He,” [1] presented to PRAC in 2008. This report includes an update to the technical plan of the experiment with cost, funding profile, and a schedule with main milestones. The goal of this experiment is to accurately measure the proton asymmetry in the reaction $\bar{n} + {}^3\text{He} \rightarrow p + T$. This experiment will use much of the NPDGamma experimental setup, making it relatively easy to construct and set up. The two main differences between the n-³He and NPDGamma experiments are: a) the target/detector, and b) running with longitudinal polarized neutrons in an effort to control systematic uncertainties. As shown in Fig. 1, the major new pieces of hardware are: a) a 10 G solenoid for the longitudinal holding field, b) a longitudinal RF spin rotator, and c) the combined ³He target / detector ion chamber.

2. Theory Developments

2.1. Few-body Calculation

A theoretical calculation of the $\bar{n} + {}^3\text{He}$ reaction in terms of DDH coupling coefficients has recently been published [2]. The calculation was performed in two steps. First the four-body scattering problem was solved using the Kohn variational method and expanding the internal part of the wave function in terms of the hyperspherical harmonic (HH) functions (for a review, see Ref. [3]). Assuming a negligible energy for the incident neutrons, they considered only $L = 0$ states. Of consequence there were only states with total angular momentum $J = 0$ or 1. In these calculations no parity mixing was considered, therefore the wave functions corresponded to the cases $J^\pi = 0^+, 0^-, 1^+, 1^-$. The wave functions were obtained for a variety of realistic models for the strong interactions, including also a 3N force model. The accuracy of these wave functions was tested by comparing the obtained n-³He scattering lengths with the values obtained by means of the Faddeev-Yakubovsky technique and the available experimental data.

¹Co-Spokesmen

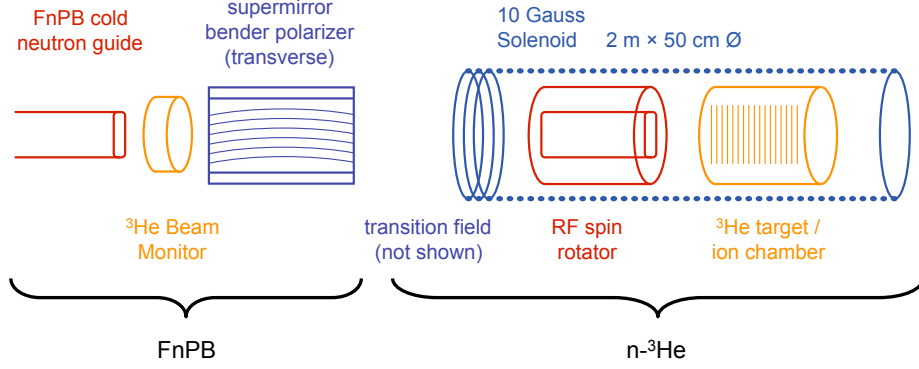


Figure 1: The n - ${}^3\text{He}$ experimental setup including existing equipment at the FnPb from the NPDGamma experiment: the supermirror polarizer and ${}^3\text{He}$ beam monitor. The radiological and magnetic shielding for the NPDGamma experiment is also adequate for the n - ${}^3\text{He}$ experiment.

In the second step, the strong interaction wave functions were used to compute the matrix element of the transition $\langle J^- | V_{PV} | J^+ \rangle$, where V_{PV} is a PV potential. The matrix elements were then combined to obtain the longitudinal observable. The calculated sensitivities to the DDH couplings shown in Table 1, and compared to those from other reactions in Table 2. Using the DDH best values range, the asymmetry is estimated to range from $A_p = (-0.944 - 2.48) \times 10^{-7}$, depending on the input strong-interaction Hamiltonian. This calculation agrees with an estimate based on microscopic theory of nuclear reactions [4].

The PISA group is currently working on a calculation within the EFT framework, and expect results within the next few months.

	C_π^1	C_ρ^0	C_ρ^1	C_ρ^2	C_ω^0	C_ω^1
AV18	-0.1892(86)	-0.0364(40)	+0.0193(9)	-0.0006(1)	-0.0334(29)	+0.0413(10)
AV18/UIX	-0.1853(150)	-0.0380(70)	+0.0230(18)	-0.0011(1)	-0.0231(56)	+0.0500(20)
N3LO	-0.1989(87)	-0.0120(49)	+0.0242 (9)	+0.0002(1)	+0.0080(30)	+0.0587(11)
N3LO/N2LO	-0.1110(75)	+0.0379(56)	+0.0194 (10)	-0.0007(1)	+0.0457(36)	+0.0408(14)

Table 1: The coefficients C_α^i entering the PV observable a_z , from [2] corresponding to the AV18, AV18/UIX, N3LO, and N3LO/N2LO strong-interaction Hamiltonians. The statistical errors due to the Monte Carlo integrations are indicated in parentheses, and correspond to a sample consisting of $\sim 130\text{k}$ configurations.

2.2. What will we learn from the \bar{n} - ${}^3\text{He}$ reaction?

Data from \bar{n} - ${}^3\text{He}$ will play a key role to achieving an important milestone in testing current understanding of the weak hadronic physics: they will allow us to test the predictive power of the DDH model in few-body systems for the first time. The following analysis is carried out in the context of the DDH model, since all of the couplings are known; however the results will apply equally to EFT once the calculations have been performed within that framework. Of the six meson couplings, the two $\Delta I = 1$ vector couplings have small DDH best values and also a small reasonable range. They are experimentally inaccessible, so we will consider the four couplings f_π , h_ρ^0 , h_ω^0 , and h_ρ^2 . Data are available for four distinct combinations of couplings: a) $\bar{p}p$ at either 15 or 45 MeV, b) elastic $\bar{p}p$ scattering at 220 MeV, c) ${}^{18}\text{F}$ circular polarization, and d) odd-p nuclei: elastic $\bar{p}{}^4\text{He}$ scattering; ${}^{19}\text{F}$, ${}^{41}\text{K}$, ${}^{175}\text{Lu}$, and ${}^{181}\text{Ta}$ circular polarization, and the ${}^{133}\text{Cs}$ anapole moment. All of the odd-p observables are proportional to the one-body weak proton-nucleus potential X_N^p [5], and all six nuclei are all consistent within the error, about 10%. ${}^{18}\text{F}$ depends only on f_π and the experimental value is zero within error. After the SNS NPDGamma experiment is complete, we will have a determination of f_π to the better precision in a completely calculable system. From the Viviani calculation, we learn that \bar{n} - ${}^3\text{He}$ has the same couplings as X_N^n . After subtracting f_π , it is sensitive to the $\Delta I = 0$ couplings. We may now make two different comparisons: a) Note that $X_N^{p;n}$ only differ by the sign of f_π . Thus we may make two direct measurements of the one-body nucleon-nuclear potential, and make a second comparison

Observable	Exp. [10^{-7}]	c_π	c_ρ^0	c_ρ^1	c_ρ^2	c_ω^0	c_ω^1
X_N^p	35 ± 2	5.5	-1.13	-4.8	0	-.91	-.77
X_N^n	(38 ± 10)	-5.5	-1.13	-4.8	0	-.91	-.77
^{18}F	$1.2 \pm 3.9 [10^4]$	3850.	0	0	0	0	0
A_L^{pp} (15 MeV)	-1.7 ± 0.8	0	0.0419	0.0419	0.0171	0.0460	0.0460
A_L^{pp} (45 MeV)	-2.3 ± 0.9	0	0.0739	0.0739	0.0302	0.0670	0.0670
A_L^{pp} (221 MeV)	$0.84 \pm .34$	0	0.0391	0.0391	0.0160	0	0.
A_L^{pd}	$-.35 \pm .85$	0.2307	0.0237	0.0098	0	0.0167	0.01256
$A_L^{p^4He}$	-3.3 ± 0.9	-0.3329	0.1395	0.0474	0	0.0586	0.05859
P_γ^{np}	1.8 ± 1.8	0	-0.0307	0	-0.0245	0.0084	0
A_γ^{np}	0.6 ± 2.1	-0.1070	0	-0.0014	0	0	0.0042
A_γ^{nd}	78 ± 34	0.6896	-0.3348	0.9905	0.0559	-0.2218	0.0544
$A_\gamma^{n^3He}$	$(1.14 \pm .33)$	-0.1892	-0.0364	0.0193	-0.0006	-0.0334	0.0413
$\frac{d\phi_n}{dz}$ (4He)	1.7 ± 9.1	0.97	0.32	-0.11	0	0.22	-0.22
fit – all data		-0.46 ± 0.92	-43.3 ± 8.8	—	37.3 ± 12.9	13.7 ± 9.4	—
fit – few-body		± 0.64	± 9.3	—	± 11.4	± 9.5	—

Table 2: Sensitivities of difference PV observables to the DDH couplings. The values in parentheses are fit from the rest of the data using fitted coupling constants, displayed in the bottom section. The last line includes only present few-body measurements and the projected NPDGamma and \bar{n}^3He errors.

of heavy nuclei with a few-body observable to the 10% level. b) with the \bar{n}^3He experiment, there will be five independent few-body observables, $\bar{p}p$ at two energies, $\bar{p}\alpha$, $\bar{n}p$, and \bar{n}^3He so we can test the internal consistency of the DDH model. The last two rows of Table 2 show the extracted couplings with the current world data including nuclei, and then the predicted uncertainties of the couplings without only few-body observables, including projected uncertainties of the NPDGamma and the \bar{n}^3He experiments. We will have a better determination of f_π , and uncertainties in the other coefficients will stay the same, but without the uncertainty of nuclear calculations.

3. Technical Feasibility

3.1. Statistical Errors

Since the last PRAC, the estimate of systematic sensitivity remains unchanged. The projected statistical error after running for 2775 hours of beam, corresponding to a one year beam cycle when efficiencies are included, is

$$\delta A = \frac{\sigma_d}{P\sqrt{N}} = \frac{6}{0.96\sqrt{2.2 \times 10^{10} \text{ n/s} \cdot 10^7 \text{ s}}} = 1.3 \times 10^{-8} \quad (1)$$

3.2. Systematic Errors

Likewise, the systematic error calculations from the last PRAC remain unchanged. As a reminder, they are listed in table 3. The technical requirements in order to control our systematic errors are summarized in table 4.

3.3. Alignment

The dominant systematic uncertainty arises from the parity-allowed $\sigma_n \cdot k_p \times k_n$ asymmetry coupled to an x or y asymmetry in the detector. If the σ_n is along x (up-down) and k_n is along z (downstream), a (left-right) asymmetry with respect to the y direction of the emitted proton exists. Hale has evaluated this asymmetry using R -matrix fits to a large body of experimental data in the mass-4 system. Hale finds $A_y(90^\circ) = 1.7 \times 10^{-6}$ at 10 meV. We wish to make the systematic uncertainty arising from this interaction less than 10^{-9} , 10% of our goal statistical uncertainty. Our strategy is:

1. Make the detector symmetric with respect to x and y . (The beam is along z .)

Invariant	Parity	Size	Comments
$\vec{\sigma}_n \cdot \vec{k}_p$	Odd	3×10^{-7}	Nuclear capture asymmetry
$\vec{\sigma}_n \cdot (\vec{k}_n \times \vec{k}_p)$	Even	2×10^{-10}	Nuclear capture asymmetry
	Even	6×10^{-12}	Mott-Schwinger scattering
$\vec{\sigma}_n \cdot \vec{B}$	Even	1×10^{-10}	Stern-Gerlach steering
	Even	2×10^{-11}	Boltzmann polarization of ^3He
	Even	4×10^{-13}	Neutron induced polarization of ^3He
$\vec{\sigma}_n \cdot \vec{k}_n$	Odd	1×10^{-11}	Neutron beta decay

Table 3: Cartesian invariants and their associated systematic uncertainties.

Property	Specification
Magnetic holding field	10 G
Field gradient (^3He neutron polarimetry)	$5 \times 10^{-4}/\text{cm}$
Field uniformity (position)	3%
Field uniformity (reversal)	1%
Field uniformity (angle)	10 mrad
Drift chamber wire plane alignment	10 mrad
Neutron beam direction alignment	10 mrad

Table 4: Specifications of fields and alignment.

2. Make σ_n along the axis of symmetry of the detector.
3. Make the average of the neutron momentum direction, k_n , parallel to σ_n .

Detector Symmetry We will build a detector that can be rotated by π about its symmetry axis. Rotating the detector reverses both x and y . If we average the proton longitudinal asymmetries taken with the two angles, the transverse asymmetry of the detector, a few %, will be reduced by more than 100.

Spin Direction The direction of σ_n is along the guide field direction because the neutron spin adiabatically follows the guide field. The guide field will be aligned to the detector axis of rotation to within 1 mrad with the detector rotation axis using a wind-blown generator invented by Vant-Hull and Henrickson. The wind-blown generator consists of a aluminum sphere mounted in a hollow aluminum cube. The axis of the sphere has a shaft that is mounted along one of the diameters of the cube. The sphere has a hole drilled through it normal to the rotation axis. The rotation is driven by compressed air. The rotation of the sphere in an ambient field produces eddy currents around the hole in the sphere. The fields produced by the currents are detected by x and y pick-up windings and demodulated by a lock-in amplifier synchronized by a LED viewing a light through the hole. This device was used by Vant-Hull and Mercerau to minimize the magnetic fields inside superconducting shields. We will align the axis of rotation of the generator with that of the detector. The x and y components of the magnetic field will be nulled by observing the x and y components of the pick-up coils. Six of these devices were built at Caltech in the mid 60's. Vant-Hull has generously agreed to provide a generator to the n-3He experiment. Nulling out the transverse fields will reduce the false asymmetry by a factor of 100–1000.

Average Momentum Direction We have built a scanning current-mode neutron detector for use in the NPDGamma experiment. A neutron beam impinges on a 1 inch diameter 0.1 inch thick B_4C disk. Ninety-four percent of the neutrons are converted to 0.488 MeV gammas. The gammas are detected in a CsI crystal viewed by a vacuum-photo-diode. The diode current is amplified by a low-noise I to V preamp. The crystal is protected from the beam by a layer of ^6Li plastic between the B_4C disk and the crystal. A ^6Li leaf can be remotely placed over the B_4C disk to measure the diffuse neutron and gamma backgrounds in situ. The entire detector system can be scanned in x and y by a stage driven by stepping motors. The absolute neutron

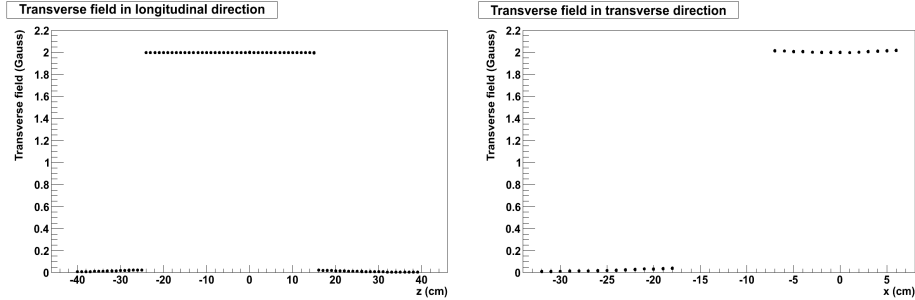


Figure 2: Field map of double-square-cosine-theta-coil constructed for nEDM experiment. a) along centerline, b) transverse cut near the center of the coil.

detection efficiency of the detector is measured using a ^{137}Cs source of known strength. The x and y scans determine the centroids and intensity of the beam and the absolute beam intensity. Measuring the centroids of the beam with an accuracy of 1% at two values of z differing by 1 meter determine the average angle of the beam with an uncertainty of 2 mrad. Combining these three reduction factors reduces the maximum, 10^{-5} , false asymmetry by a factor of 10^{-7} . The resulting false asymmetry is completely negligible.

3.4. Radiological issues

The primary source of radiation for the n- ^3He experiment is the exit of the guide and the polarizer. These will have already been addressed for the NPDGamma experiment and simulations show that the HD concrete tunnel plus the lead collimator/wall at the end of it contain the radiation sufficiently that the dose external to the BL13 cave is within mandated levels.

A secondary source of radiation is due to scattering of neutrons from air in the flight path between the polarizer and the target/detector. This has again been addressed for NPDGamma with the installation of an aluminum tube lined with ^6Li enriched lithium carbonate loaded plastic sheets. Capture in the air is not a significant issue but preventing scattered neutrons from reaching the cave walls and roof is. Simulations have confirmed that this tube solves the problem.

Scattering of neutrons from the ^3He target/detector is unlikely to be significant. If calculations suggest otherwise, the outside can be encased in the same ^6Li enriched lithium carbonate loaded plastic sheets as used for the drift tube.

Finally, there will be a significant production of ^3H during the course of this experiment. One suggested method of confining it to a localized volume is via a passive loop containing a vessel with chips of depleted Uranium to act as a getter. Upon completion of the experiment, essentially all of the tritium would be absorbed in the getter which could be disposed of appropriately. Note that as long as the system remains closed, there is no radiological hazard to personnel in the vicinity. The 14 keV electrons from tritium beta-decay cannot penetrate the walls of the vessel.

4. Updates in Experimental Design

4.1. RF Spin Rotator

Since the last PRAC, one prototype magnet has been constructed and tested using our magnetic scalar potential method [6]. The magnet was built as a prototype for the nEDM guide field at the end of the neutron guide. It was constructed out of PCB board with traces cut by CNC router, with the traces on individual traces soldered together at the corners to form complete traces. On axis the prototype agreed with calculations to 1% (see the field map in Fig. 2). Near the end, discrepancies between the calculated and measured field were traced back to imperfections in the solder joints between the faces.

We have constructed a new prototype spin flipper using a nylon core with holes drilled in each endcap to place the windings at the calculated positions. For this prototype, we used cylindrical geometry, so that it forms a double cosine theta coil. The winding geometry is shown in Fig. 3, along with the simulated field $B_x(y)$ (the horizontal field in the vertical direction). This coil will be mapped both at DC as a prototype spin rotator for the NIST interferometer, and with RF as a prototype for the n- ^3He experiment. After this

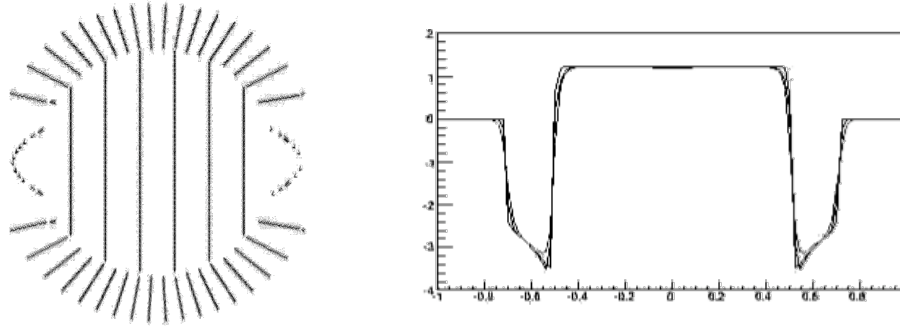


Figure 3: a) Winding geometry of the new prototype spin rotator coil. b) Calculation of the transverse field along the vertical axis, showing the uniform field region in the middle, and the flux return on the top and bottom.

prototype we will begin construction of the actual RFSF resonator.

4.2. ^3He Ion Chamber

The geometry of the ion chamber was finalized, and was delivered by Atlas Technologies. In the mean time, research and development has been carried out on the NPDGamma beam monitors. Fig. 4 shows the design drawing for the wire chamber.

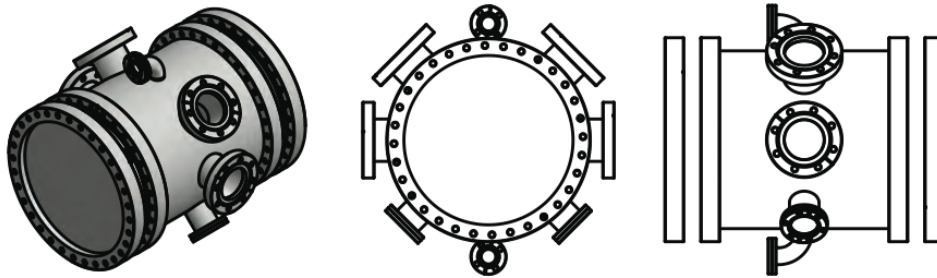


Figure 4: Design of the target / ion chamber.

5. Organization, Cost, and Schedule

The $n\text{-}^3\text{He}$ experiment held its first collaboration meeting, on 2010-10-16. The list for work package leaders was formalized at the meeting.

The cost estimate from the previous review is given in Table 6. The project has funding through NSERC (Canada) for the detector, and CONACYT (Mexico) for the solenoid. An 5-year grant application has been submitted to the DOE to fund the spin rotator, DAQ system, and a graduate student and postdoc to work on the experiment, and is pending review.

The milestones presented at the last review are shown in Table 7. For the target dates that have passed: a) Prototypes have been developed for the RFSF, but the final design has not been built; and b) parts have been acquired for the target / ion chamber. Acquisition of the DAQ system, and student support for construction and testing of the RFSF (and DAQ) have been delayed until funds are available to support these activities.

6. Summary

The critical progress made this year includes finalization of the calculation to sensitivity in the DDH framework, development of the RFSF, acquisition of parts for the target / ion chamber, and development of

	Work Package	Work Package Leader
1	Theory	Michele Viviani
2	MC Simulations	Michael Gericke
3	Polarimetry	Stefan Baessler / Matthew Musgrave
4	Beam Monitor	Rob Mahurin
5	Alignment	David Bowman / Geoff Greene
6	Field Calculation	Septimiu Balascuta
7	Solenoid / fieldmap	Libertad Baron Palos
8	Transition, trim coil	Pil-Neyo Seo
9	RFSF	Chris Crawford
10	Target / detector	Michael Gericke
11	Preamps	Michael Gericke
12	DAQ	Nadia Fomin / Chris Crawford
13	Analysis	Nadia Fomin / Chris Crawford
14	System integration/CAD	Seppo Penttilä
15	Rad. Shielding / Tritium	John Calarco

Table 5: Top-level subproject structure, responsible institutions, and responsible persons.

	Subproject	Base Cost	Overhead	Contingency	Total	Funded
1	Polarized beam	4	3	2	9	0
2	Spin flipper	16	3	6	25	0
3	Magnetic field	45	17	18	80	25
4	Target/detector	113	6	34	153	134
5	DAQ system	94	24	31	149	0
6	Shielding/collimation	7	2	2	11	0
7	Alignment	5	3	2	12	0
8	Operation	5	3	2	12	0
	Total	298	66	97	451	159

Table 6: Estimated base costs of each subproject, calculated overhead and contingency, and received funds [k\$].

a new alignment strategy. International collaborators have secured a significant fraction of the equipment funds, and the remaining large ticket items have been requested from DOE.

References

1. n-³He 2008 PRAC Proposal:
http://www.pa.uky.edu/~crawford/pub/n3he_proposal_sns.pdf
<http://www.physics.umanitoba.ca/~mgericke/n3He/Proposal.pdf>
2. M. Viviani, R. Schiavilla, L. Girlanda, A. Kievsky and L. E. Marcucci, Phys. Rev. C 82, 044001 (2010), arXiv:1007.2052 [nucl-th].
3. A. Kievsky *et al.*, J. Phys. G: Nucl. Part. Phys. **35**, 063101 (2008).
4. V. Gudkov, Parity violation in n + ³He → H + p reaction: resonance approach, to be submitted.
5. B. Desplanques, Phys. Rep. **297**, 1 (1998).
6. E. Martin, C.B. Crawford, “A Double Cosine Theta Coil Prototype”, nEDM technical report, Oct. 28, 2010.

Subproject	Milestone	Date
2a	RFSF resonator designed	Jan 2010
2b	RFSF resonator constructed	July 2010
2c	RFSF tested with polarized neutrons	Dec 2010
3a	Magnetic system designed	April 2010
3b	Solenoid constructed	Jan 2011
4a	Finished chamber design	Dec 2009
4b	Finished wire frame design and wire trace layout design	Mar 2010
4c	Chamber procured through Atlas Technologies	Mar 2010
4d	Completion of procurement for all parts	Sept 2010
4e	Completion of wire frame parts	Sept 2010
4f	Completion of wire frame assembly with wires	Mar 2011
4g	Completion of chamber assembly and testing	June 2011
5a	DAQ system components procured	July 2010
5b	DAQ software written and tested on bench	Jan 2011
1a	Initial neutron polarization measurement	June 2011
1b,7a	Measurement of neutron beam angle	June 2011
3c	Solenoid installed	July 2011
3d,7b	Initial field mapping	Aug 2011
4h,7c	Chamber installed and surveyed	Sept 2011
6a	Shielding installed	Sept 2011
8a	Experiment installed, ready to commission	Oct 2011
8b	Data taking for transverse polarization	Nov 2011
8c	Data taking for longitudinal polarization	Jan 2012
8d	Completion of data-taking	Dec 2012
1c	Final neutron polarization measurement	Dec 2012
8e	Data analyzed and published	Dec 2013

Table 7: Project milestones from previous report. Independent subsystem construction milestones are grouped by subsystem, followed by interdependent milestones during integration and data taking at the FnPB.